Cerebral Cortex, 2018; 1–12

doi: 10.1093/cercor/bhx334
Original Article

ORIGINAL ARTICLE

The Roles of Subdivisions of Human Insula in Emotion Perception and Auditory Processing

Yang Zhang[1], Wenjing Zhou[2], Siyu Wang[2], Qin Zhou[2], Haixiang Wang[2], Bingqing Zhang[2], Juan Huang[3], Bo Hong[1] and Xiaoqin Wang[1,3]

[1]Tsinghua Laboratory of Brain and Intelligence (THBI) and Department of Biomedical Engineering, Tsinghua University, Beijing 100084, P.R. China, [2]Department of Epilepsy Center, Tsinghua University Yuquan Hospital, Beijing 100040, P.R. China and [3]Department of Biomedical Engineering, The Johns Hopkins University, Baltimore, MD 21205, USA

Address correspondence to Xiaoqin Wang, PhD, Tsinghua Laboratory of Brain and Intelligence, Tsinghua University, Beijing 100084, China. Email: xiaoqinwang@tsinghua.edu.cn; Bo Hong, PhD, Department of Biomedical Engineering, Tsinghua University, Beijing 100084, China. Email: hongbo@mail.tsinghua.edu.cn

Abstract

Previous studies have shown insular activations involving sensory, motor, and affective processing. However, the functional roles of subdivisions within the human insula are still not well understood. In the present study, we used intracranial electroencephalography and electrical cortical stimulation to investigate the causal roles of subdivisions of the insula in auditory emotion perception in epilepsy patients implanted with depth electrodes in this brain region. The posterior and the anterior subdivisions of the human insula, identified based on structural and functional analyses, showed distinct response properties to auditory emotional stimuli. The posterior insula showed auditory responses that resemble those observed in Heschl's gyrus, whereas the anterior insula (AI) responded to the emotional contents of the auditory stimuli in a similar way as observed in the amygdala. Furthermore, the degree of the differentiation between various emotion types increased from the posterior to the AI. Our findings suggest different roles played by the two regions of the human insula and a transformation from sensory to affective representations in auditory modality along the posterior-to-anterior axis in the human insula.

Key words: auditory processing, emotion perception, insula

Introduction

The human insula, which lies deeply inside the Sylvian fissure under the frontal, parietal, and temporal opercula, contains 5–7 gyri and can be divided into anterior and posterior regions by the central insular sulcus (Mesulam and Mufson 1985; Flynn 1999). In cytoarchitectonic and myeloarchitectonic studies (Augustine 1996; Rivier and Clarke 1997), the insular cortices of human and nonhuman primates can be divided into 3 major areas from posterior to anterior based on cytoarchitectonic features, which include posterior granular, middle transitional dysgranular, and anterior agranular areas (Rose 1928; Mesulam and Mufson 1982, 1985). Tracing studies in nonhuman primates have revealed dense connections between the posterior granular insula and thalamic nuclei complexes, including the medial geniculate body (Burton and Jones 1976; Jones and Burton 1976) and between the anterior agranular insula and the orbitofrontal cortex (von Economo and Koskinas 1925; Allman et al. 2010). In addition, the insula has abundant intra-insular connections (Mesulam and Mufson 1982, 1985; Augustine 1996) and extensive reciprocal interconnections with the amygdala (Aggleton et al. 1980; Turner et al. 1980; Mufson et al. 1981; Mesulam and Mufson 1982, 1985; Augustine 1985; Höistad and Barbas 2008) and auditory

cortex (Pandya et al. 1971; Augustine 1985; Mesulam and Mufson 1985; Pandya and Rosene 1985).

More recently, researchers have used diffusion tensor imaging (DTI) (Cerliani et al. 2012; Cloutman et al. 2012; Dennis et al. 2014) and resting state functional magnetic resonance imaging (fMRI) (Cauda et al. 2011; Nomi et al. 2016) techniques to reveal functional connectivity of the insula in the intact brain. Using these methods, researchers have identified 2 complementary networks involving the anterior and the posterior insula (PI) in which the anterior insula (AI) connects to the frontal cortex, the cingulate cortex, and the amygdala and the PI connects to the premotor, sensorimotor, visual, and auditory cortices.

Previous functional imaging and electrical stimulation studies in humans and nonhuman primates have suggested that subdivisions within the insula have different functions. For example, the PI has been suggested to be involved in processing sensorimotor (Ostrowsky et al. 2002), auditory (Bamiou et al. 2003; Remedios et al. 2009; Chen et al. 2014), and visual information (Augustine 1996), whereas the AI is involved in processing affective information (Phan et al. 2002; Barrett and Wager 2006; Lamm and Singer 2010; Caruana et al. 2011; Zaki et al. 2012). Craig (2009) proposed a posterior-to-anterior functional gradient within the insula, from primarily interoceptive representations in the PI to higher subjective awareness representations in the AI. However, there has been little evidence to validate this proposed model. In addition, the functions of the AI and the PI in processing auditory information and emotional contents carried by auditory stimuli remain largely unknown.

In the present study, we investigated the functional roles of subdivisions within the human insula in processing auditory information and emotional information from the auditory modality using structural and functional data obtained from epilepsy patients. We obtained DTI and resting fMRI data to identify subdivisions of the insula in each subject. Intracranial electroencephalography (iEEG) signals were recorded from the electrodes located in the insula and other brain areas while a subject was presented with emotional and nonemotional sounds and performed auditory emotion recognition tasks. The iEEG responses obtained from the insula were compared with those obtained from the Heschl's gyrus (HG) and the amygdala to reveal auditory and emotion processing across subdivisions of the insula. In addition, we obtained electrical stimulation data from the same subjects to validate the proposed functional roles of the insula subdivisions. Our overarching hypothesis is that there is a transformation from sensory to affective representations in auditory modality along the posterior-to-anterior axis in the human insula. The findings of this study provide new insights for a sensory/affective dissociation in subdivisions of the human insula.

Materials and Methods

We collected DTI, resting fMRI, and iEEG data from 24 epilepsy patients (see Supplementary Table S1, mean age: 24.7, age range: 13–47, 14 males and 10 females) and electrical cortical stimulation (ECS) data from 41 epilepsy patients, which included the 24 patients from whom DTI, resting fMRI, and iEEG data were collected (see Supplementary Table S2, mean age: 24, age range: 13–47, 23 males and 18 females). The first 24 patients in Supplementary Table S2 are identical to those listed in Supplementary Table S1. As a control, we also collected DTI data from 30 normal subjects (mean age: 29.7, age range: 20–46, 4 males and 26 females). We did not collect resting fMRI data from normal subjects because such data are available in previously published studies (Cauda et al. 2011; Nomi et al. 2016) that showed similar results as the resting fMRI data that we collected from the patients in this study. The patients were all implanted with intracranial depth iEEG electrodes (0.8-mm electrode diameter and 3.5-mm interelectrode center-to-center distance) as part of their clinical treatment for epilepsy. All subjects were right-handed with a normal IQ and normal hearing. Written informed consent was obtained for each subject before participation. The experimental protocol was approved by the Institutional Review Board at Tsinghua University and the affiliated Yuquan Hospital.

DTI and Resting fMRI Data

DTI and resting fMRI data were acquired using a Philips Achieva 3.0 T TX scanner equipped with a 16-channel head coil. First, one high-resolution (1-mm isotropic) 3D anatomical scan (T1, matrix size: 256 × 256, 180 slices) was acquired. DTI data were acquired using a single-shot, pulsed gradient spin echo planar (EPI) sequence (TR = 6800 ms, TE = 69 ms, flip angle = 90°, slice thickness = 2 mm), with each volume consisting of 60 transverse slices, and the analyses were performed along 33 independent directions, including a b-value of 1000 s/mm^2. Subjects were instructed to keep their eyes closed, think of nothing, and not to fall asleep during the resting fMRI scan. The images were acquired using EPI sequences (TR = 2000 ms, TE = 30 ms, flip angle = 90°, voxel size = 3 × 3 × 3 mm^3). A total of 240 volumes were acquired in 2 separate runs, with each volume consisting of 37 transverse slices, parallel to the anterior–posterior (AC–PC) commissure. Each run lasted 8 min.

DTI data were processed and analyzed using the FSL software package (www.fmrib.ox.ac.uk/fsl), which is implemented in the "PANDA" toolbox in MATLAB (Cui et al. 2013). To compare the connection patterns of the subdivisions of the insula, we used the Human Brainnetome Atlas (Fan et al. 2016) to divide the insula into 6 subdivisions (Fig. 1A) and then tracked the connections of these 6 subdivisions with other cortical areas separately. We chose auditory, visual, sensorimotor, frontal cortices, and the amygdala as the target regions and insular subdivisions as the seed regions. Auditory cortices included superior temporal gyrus. Visual cortices included medioventral occipital cortex and lateral occipital cortex. Sensorimotor cortices included precentral gyrus and postcentral gyrus. Frontal cortices included superior, middle, and inferior frontal gyri. We performed probabilistic fiber tracking between insular subdivisions and target regions (see Supplementary Materials). Statistical analyses were performed across subjects with Bonferroni corrections.

Resting fMRI (Hampson et al. 2002; Greicius et al. 2003; Fox et al. 2005; Damoiseaux et al. 2006; Vincent et al. 2007) data were analyzed using MATLAB and Freesurfer software (http://surfer.nmr.mgh.harvard.edu/). Functional images were preprocessed as follows to reduce artifacts (Wang et al. 2015): 1) slice timing correction, 2) 3D motion correction, 3) normalization for global mean signal intensity across runs, 4) spatial smoothing using a Gaussian kernel of 5 mm FWHM (full-width at half-maximum), and 5) bandpass temporal filtering (0.01–0.08 Hz). Then, the preprocessed data were registered to fsaverage brain and subjected to a voxelwise fuzzy clustering technique. The insula was then classified into two clusters (Cauda et al. 2011). In addition, we computed functional connectivity maps of these two clusters to other cortical areas using the Pearson correlation. We considered the Fisher transforms of the correlation

map of the single voxel in the insula as a distribution for calculating the Z-score. The Z-scores were then averaged across the 24 patients, cluster threshold $k > 10$.

iEEG Data

Stimuli and Task

Stimuli consisted of emotional and nonemotional sounds. The nonemotional sounds included noise, 2 pure tones (PT), 2 harmonic tones (Harm), Chinese speech /yi/ with 3 different pitch contours (yi(2), yi(1), and yi(4)), /da/, and phase-scrambled /da/. The emotional sounds were taken from the Montreal Affective Voices (Belin et al. 2008), in which actors or actresses were instructed to produce the vowel /a/ with different emotional interjections. Voices from 2 identities (1 male and 1 female) expressing 6 emotions (anger, fear, disgust, happy, sad, and neutral) were chosen in this study. All stimuli were normalized to the same sound level, were controlled by MATLAB (The Mathworks, Natick, MA, USA) using the Psychophysics Toolbox 3.0 extension (Brainard 1997), and were delivered via insert air-conduction earphones. The volume was adjusted to a comfortable level of approximately 65 dB sound pressure level. All stimuli were presented in a randomized order, and each was repeated 20 times. Subjects needed to identify the emotion type of the sound they heard by pressing a button after the stimulus was over using the hand ipsilateral to the side of the electrodes coverage.

iEEG Data Acquisition

iEEG signals were recorded via a 256-channel Neurofax EEG-1200c amplifier/digitizer system (Nihon Kohden, Japan) from implanted depth electrodes with a high-pass filter of 0.01 Hz cut-off frequency, a notch filter at 50 Hz, and a sampling rate of 2000 Hz. Electrodes placed on the inner surface of the skull were used as the ground and reference.

Electrode Localization

We only focused on electrodes that had contacts in the insula, HG, and the amygdala. The locations of the electrodes relative to the cortical surface were determined using Freesurfer. We reconstructed the individual brain's 3D map with electrode locations on the surface by aligning the presurgical high-resolution, T1-weighted MRI obtained with a Philips Achieva 3.0 T TX scanner with the postsurgical computed tomography (CT) images obtained using the Siemens SOMATOM Sensation 64 CT scanner. This registration was visually verified and manually adjusted if necessary. To show all subjects' implanted electrodes on an average brain surface, we coregistered the individual MRIs to the fsaverage brain through Freesurfer software, and all electrodes were displayed on a 3D-constructed cortical surface representing the average brain. Furthermore, the electrode locations were also superimposed onto the inflated average brain for visualization. We analyzed electrodes from the HG, the PI, the AI, and the amygdala separately. HG, insula, and amygdala were defined and dissociated according to the anatomic labels of the average brain in Freesurfer software. The PI and the AI were defined and dissociated according to the fMRI-clustering results.

iEEG Data Analysis

All analyses were performed in MATLAB. Each channel was visually inspected for artifacts. Channels with epileptiform activity were excluded from further analysis. We used notch filters from Fieldtrip software (http://www.fieldtriptoolbox.org/) to remove 50-Hz noise and its second and third harmonics, and the data were down-sampled at 500 Hz. The data were then segmented into a 200-ms prestimulus baseline and an 800-ms poststimulus interval. All analyses focused on high-gamma response (70–140 Hz). We used the term "following/broadband response" in order to separate the phase-locking components from the typical high-gamma (70–140 Hz) responses. The Z-score of the high-gamma band was estimated using the following steps: 1) a 100-ms moving window (20-ms step) was used to perform short-time Fourier transform for the preprocessed iEEG signal, 2) each frequency component time series was then normalized to its own baseline mean and was divided by its own baseline standard deviation to determine its own Z-score time series, 3) finally, Z-score time series of the "following response" were averaged inside the range between F_0 and 10 Hz and F_0 + 10 Hz (F_0: fundamental frequency of the sound stimulus), whereas the average of the remaining frequency components in the high-gamma band range produced the Z-score time series of the broadband response. These normalization procedures sought to cancel the 1/frequency decay of power in the spectrum.

For each electrode, we defined the broadband response amplitude of each emotion type as the peak response of the broadband response Z-score time series (200-ms prestimulus to 800-ms poststimulus). "Response amplitude" refers to the mean broadband response amplitude of responses to the emotional stimuli recording from an electrode, which reflects the average response amplitude of single electrode to all emotional stimuli. To quantify the emotion-selective capacity of single electrodes, we defined the emotion selectivity index (SI) as:

$$\mathrm{SI}_i = \frac{r_i^+ - r^-}{r_i^+ + r^-},$$

where r^- is the mean broadband response amplitude to nonemotional sounds, and r_i^+ is the mean broadband response amplitude to type i emotional sounds.

SI measured the response distance between the emotional and nonemotional sounds. For visualization, the SI values were all mapped onto the inflated average brain using MATLAB. We conducted statistical analyses to compare the SI between different sites (HG, PI, AI, and amygdala) and different hemispheres by 2-sample t-test with Bonferroni corrections.

We defined a responsive trial if the Z-score of that trial exceeded the 95% confidence interval of the prestimulus baseline mean and was maintained for at least 100 ms. The latency was defined as the peak latency of each responsive trial (see Supplementary Materials).

To quantify the dissimilarity of neuronal responses elicited by different types of emotion, we used Euclidean distance to measure the pair-wise dissimilarities across electrodes in the HG, the PI, the AI, and the amygdala and obtained the confusion matrices. In these confusion matrices, larger distances between the emotion pairs indicated higher dissimilarities of their neural responses. We then defined the normalized response distance as the average distance across all emotion pairs in HG, PI, AI, and the amygdala (see Supplementary Materials).

ECS Data

In the clinical setting, the stimulation protocol sought to identify areas that caused typical seizure sensations and to map

important functional areas that needed to be preserved during surgery. A symmetric bipolar square wave electric stimulation was delivered to 2 adjacent electrodes. Every stimulation trial contained a pulse train (0.3 ms width, 0.2–8 mA) at a frequency of 50 Hz for 1–5 s. Subjects were instructed to recount any perceptual effects or changes during or after each trial. We classified the subjects' subjective reports into 5 categories (see Supplementary Table S3): 1) auditory responses, 2) sensorimotor responses, 3) autonomic responses, 4) sign of seizure, and 5) other. We focused on analyses of the first 3 categories.

Results

Structural Connections Between the Insula and Other Brain Areas Revealed by DTI

We collected DTI data from 24 epilepsy patients (see Supplementary Table S1). As a control, we also collected DTI data from 30 normal subjects. Figure 1A shows an example parcellation of the 6 subdivisions of the insula in 1 epilepsy patient (see Materials and Methods). Figure 1B shows example connection patterns between the 6 subdivisions of the insula and other brain areas in the same patient. The connections of the 6 subdivisions of the insula with other cortical areas were analyzed for both normal subjects and epilepsy patients in both hemispheres (Fig. 1C). We focused on the analysis of the connections between the insula and auditory, visual, sensorimotor, and frontal cortices and the amygdala. We performed paired *t*-test with Bonferroni corrections to compare the connection probability between subdivisions of the insula and target region across subjects. The connection probability from seed region *i* to target region *j* was defined by the number of fibers passing through region *j* divided by total number of fibers sampled from region *i* (Cui et al. 2013). We found that the hypergranular insula (subdivision 1) and the ventral dysgranular and granular insula (subdivision 3) have significant connections ($P < 0.005$) with the auditory cortex in both normal subjects and epilepsy patients (Fig. 1C, first row). The ventral dysgranular and granular insula (subdivision 3) showed significant connections ($P < 0.005$) with the visual cortex in both normal subjects and

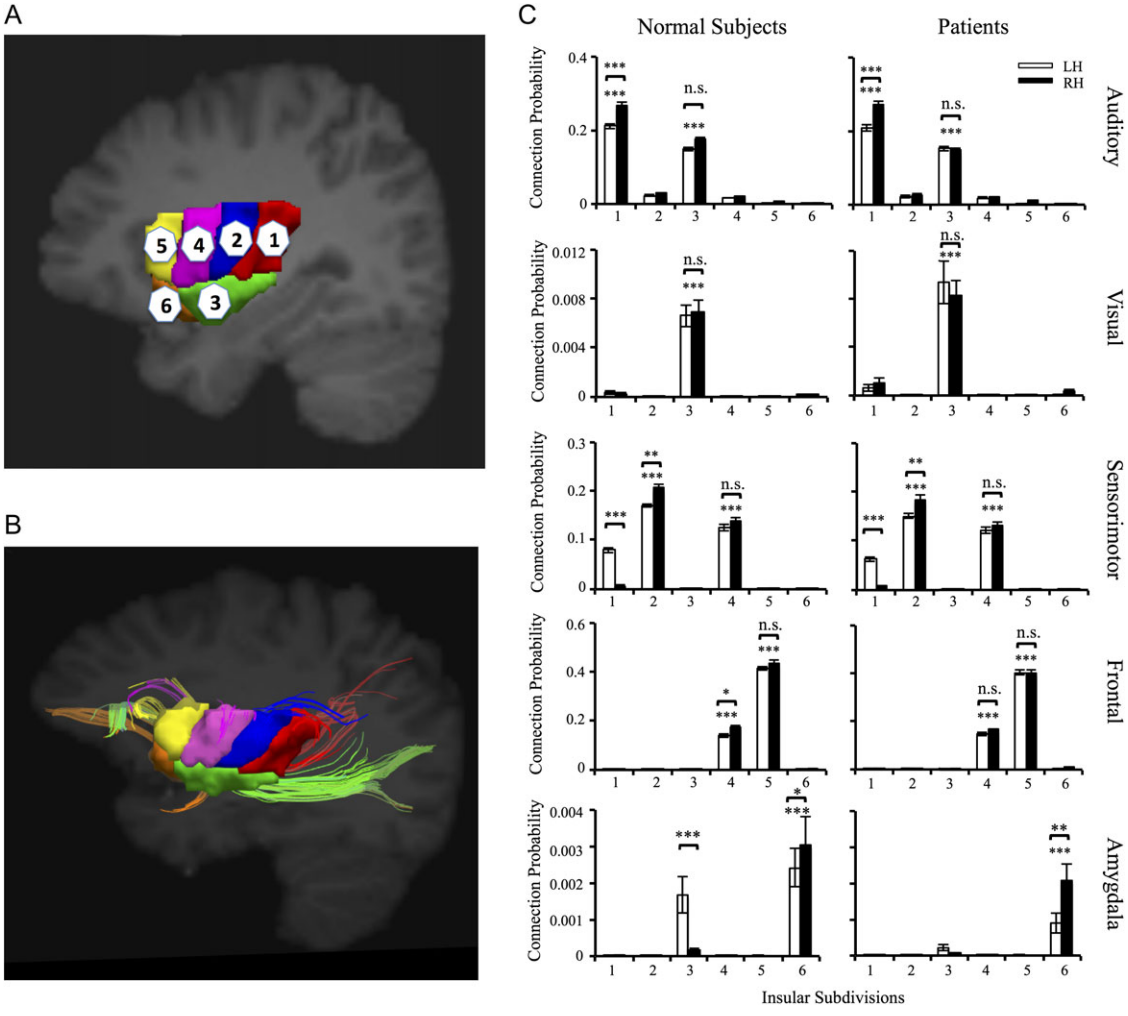

Figure 1. Probabilistic fiber pathways of normal subjects and epilepsy patients: (*A*) regions of interests were selected based on Human Brainnetome Atlas (Fan et al. 2016), which divide the insula into 6 subdivisions, as labeled from 1 patient (1: hypergranular insula; 2: dorsal granular insula; 3: ventral dysgranular and granular insula; 4: dorsal dysgranular insula; 5: dorsal agranular insula; and 6: ventral agranular insula). (*B*) Example fiber tracking of the 6 subdivisions of the insula from the same patient in (*A*). (*C*) Connection probability between the 6 subdivisions of the insula and various brain areas. Left column: normal subjects; right column: epilepsy patients. From top to bottom: connections to auditory cortex, visual cortex, sensorimotor cortex, frontal cortex, and the amygdala. LH: left hemisphere; RH: right hemisphere (*: $P < 0.05$; **: $P < 0.01$; ***: $P < 0.005$, paired *t*-test, n.s.: not significant).

epilepsy patients (Fig. 1C, second row). The dorsal granular insula (subdivision 2) and the dorsal dysgranular insula (subdivision 4) showed significant connections ($P < 0.005$) with the sensorimotor cortex in both normal subjects and epilepsy patients (Fig. 1C, third row). The dorsal dysgranular insula (subdivision 4) and the dorsal agranular insula (subdivision 5) showed significant connections ($P < 0.005$) with the frontal cortex in both normal subjects and epilepsy patients (Fig. 1C, fourth row). Finally, the ventral agranular insula (subdivision 6) showed significant connections ($P < 0.005$) with the amygdala in both normal subjects and epilepsy patients and the ventral dysgranular and granular insula (subdivision 3) showed significant connections with the amygdala only in normal subjects (Fig. 1C, fifth row). These results showed that the PI (subdivisions 1, 2, and 3) is predominantly connected with sensory cortices (auditory, visual, and sensorimotor cortex), whereas the AI (subdivisions 4, 5, and 6) is predominantly connected with the frontal cortex and the amygdala. Such a connectivity pattern indicates the potential functional differences of these two regions of the insula. The similar connectivity patterns between normal subjects and epilepsy patients suggest that the neural physiology data recorded in the insula from this group of patients are suitable for studying the functions of the insula.

Furthermore, we conducted statistical analyses to compare the differences of connection probability between left and right hemispheres (Fig. 1C). We found that the right hypergranular insula (subdivision 1 of right hemisphere) showed significant stronger connections ($P < 0.005$, paired t-test) with auditory cortex than left hypergranular insula (subdivision 1 of left hemisphere) in both normal subjects and patients. Left hypergranular insula (subdivision 1 of left hemisphere) showed significant stronger connections ($P < 0.005$, paired t-test) with sensorimotor cortex than right hypergranular insula (subdivision 1 of right hemisphere) in both normal subjects and patients. Right dorsal granular insula (subdivision 2 of right hemisphere) showed significant stronger connections ($P < 0.01$, paired t-test) with sensorimotor cortex than left dorsal granular insula (subdivision 2 of left hemisphere) in both normal subjects and patients. Right ventral agranular insula (subdivision 6 of right hemisphere) showed significant stronger connections ($P < 0.05$, paired t-test) with the amygdala than left ventral agranular insula (subdivision 6 of left hemisphere) in both normal subjects and patients. Such connection differences between left and right hemispheres may indicate functional differences of the left and right insula.

Functional Connectivity and Partition of the Insula Based on Resting fMRI Data

Resting fMRI data were collected from the same group of epilepsy patients (see Supplementary Table S1). We subjected insular fMRI data to a voxelwise fuzzy clustering algorithm (Smolders et al. 2007). The number of clusters was fixed to 2, as suggested in a previous study (Cauda et al. 2011). We then performed 2-category clustering and produced 2 subregions of the insula (Fig. 2A): one in the anterior and the other in the posterior region of the insula bilaterally. These two regions were used for separating iEEG electrodes into 2 groups (Fig. 2B). Finally, functional connectivity maps were computed for each insular subdivision with the cerebral cortex using the Pearson correlation. We did not calculate the corrections between the insula and the subcortical regions because of the low SNR of the fMRI signal in the subcortical regions. The PI in both the left and right hemispheres connected to visual, auditory, and sensorimotor cortices (Fig. 2C), whereas the AI in both the left and right hemispheres connected to frontal, anterior temporal, and cingulate cortices (Fig. 2D). These results further suggest the differences of functional connectivity pattern between the PI and AI.

Taking DTI and resting fMRI data together, we could define the structural and functional connections between the insula and other cortical areas. Figure 2E shows a schematic diagram of connections between insular subdivisions and other brain areas. We mapped 6 subdivisions of the insula defined by DTI results onto the PI and AI defined by fMRI-clustering results and found that sensory cortices, including auditory, visual, and sensorimotor, are connected to the PI, whereas the frontal cortex and amygdala are connected to the AI. We analyzed functional data from the PI and AI separately in the following sections.

Activation Patterns of Single iEEG Electrodes in Response to Emotional and Nonemotional Sounds

We also recorded iEEG signals from the same group of 24 epilepsy patients implanted with depth electrodes while they listened to emotional and nonemotional sounds (see Supplementary Table S1). Supplementary Figure S1 shows the fundamental frequencies (F_0) of the sounds used as stimuli. The analyses of iEEG data focused on high-gamma band activity (70–140 Hz). Figure 3A shows examples of responses to the sound stimulus with the "disgust" emotion ("disgust (2)" in Supplementary Fig. S1) recorded from electrodes placed in HG, PI, AI, and the amygdala, respectively. The HG and PI electrodes showed much stronger responses than electrodes in the AI and the amygdala, and interestingly, the responses of electrodes in HG and the PI tracked the fundamental frequency F_0 (white line in Fig. 3A) of the stimuli (Fig. 3A). To separate this tracking response pattern from typical high-gamma responses, we divided the response into two parts: following response (energy between F_0 and 10 Hz and F_0 + 10 Hz) and broadband response (total high-gamma response minus the following response). Supplementary Figure S2 shows the Z-score responses of all recorded electrodes to all stimuli (the upper panel shows the following response and the lower panel shows the broadband response). Electrodes in the insula were divided into PI and AI groups according to fMRI-clustering results (Fig. 2B). Electrodes located on the border between PI and AI were not included in further analyses (MI in Supplementary Fig. S1, Left: 20 electrodes; right: 25 electrodes). We found that electrodes from bilateral HG and PI have stronger following response to stimuli with F_0 of approximately 100 Hz than stimuli with other F_0. However, these results were not observed in electrodes from the AI and the amygdala (Fig. 3B). In addition, we calculated the percentage of following response energy within the total high-gamma response energy (70–140 Hz) of all recorded electrodes in HG, the PI, the AI, and the amygdala (Fig. 3C) and found that the PI has the highest percentage of following response, higher than HG, whereas the AI has less, and the amygdala has the least. The percentage of following response in PI was significant different from that in AI and the amygdala ($P < 0.01$, 2-sample t-test, Bonferroni correction). These findings indicate that similar to HG (Griffiths et al. 2010), tracking the F_0 of a sound stimulus may also be a key feature of the PI response. For broadband response, we found that HG and the PI showed significant stronger responses to nonemotional sounds than emotional stimuli in both left and right hemispheres ($P < 0.01$, 2-sample t-test), whereas the AI and the amygdala showed significant stronger responses to emotional stimuli than nonemotional sounds in both left and right hemispheres (Fig. 3D, $P < 0.01$, 2-sample t-test). Furthermore, we found that the latency increased from HG, the PI to the AI and the amygdala, with a prominent gap between PI and AI (Fig. 3E).

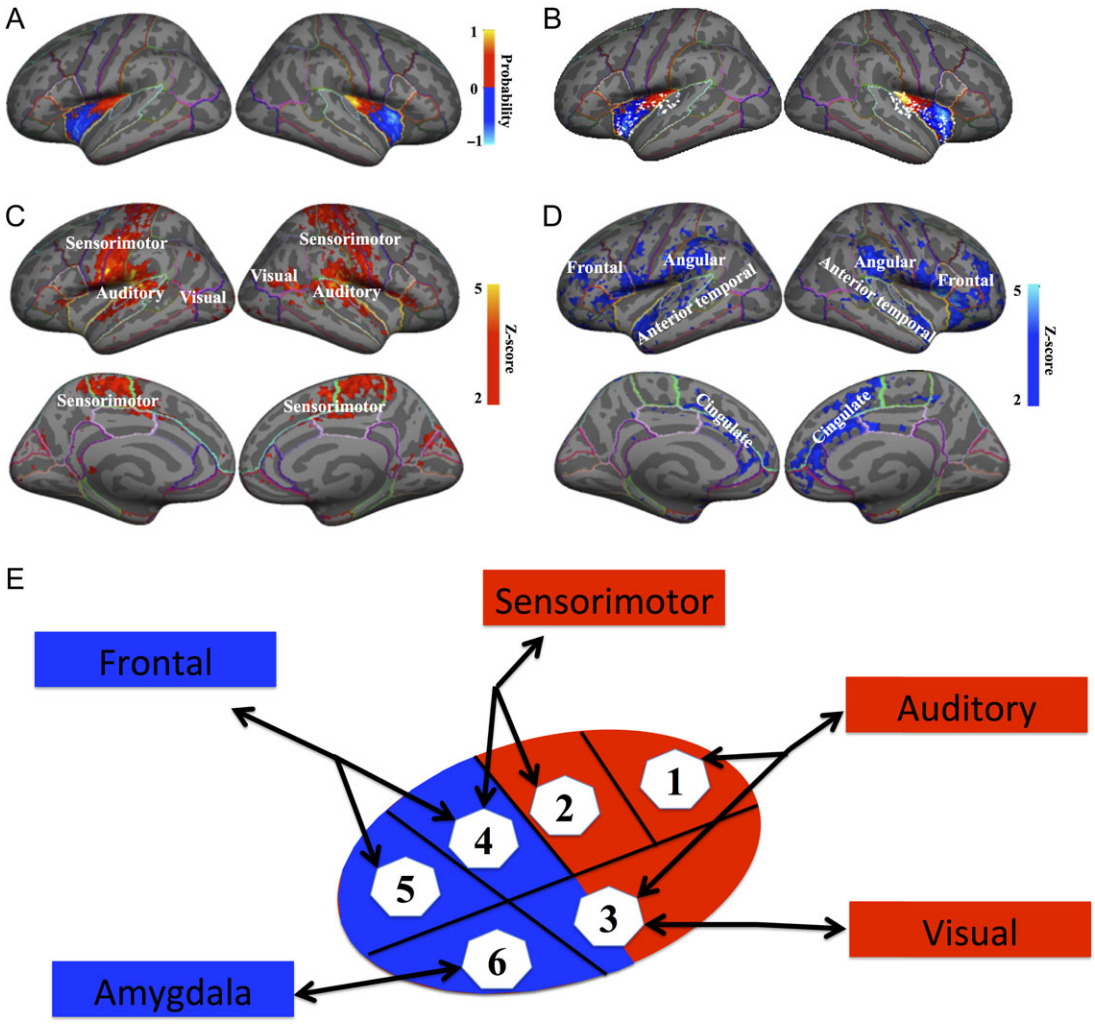

Figure 2. Voxelwise clustering and whole brain correlation maps of the insula: (*A*) Fuzzy C-means clustering of the insula into the anterior and posterior regions. The color scheme represents the probability of overlapping regions in each voxel across the 24 epilepsy patients. (*B*) Mapping the locations of the iEEG electrodes onto the clustering of the insula, separating the electrodes into anterior and posterior groups. (*C*) Correlation maps of the PI with other cortical areas. (*D*) Correlation maps of the AI with other cortical areas. (*E*) Schematic diagram of the insular connections with other brain areas based on DTI and resting fMRI data (1–6: insular subdivisions from DTI results, red: PI, blue: AI).

Emotion Selectivity in HG, the Insula, and the Amygdala

Given the response patterns found from single electrodes, we sought to quantify the emotion SI of every single electrode. SI measured the response distance between emotional and non-emotional sounds. We found that similar to HG, the PI had no emotion selectivity, whereas the AI and the amygdala showed strong emotion selectivity (Fig. 4A, SI of the AI and the amygdala were significant different from SI of the HG and the PI, $P < 0.005$, Fisher transform, 2-sample *t*-test, Bonferroni correction). This trend was also found for all types of emotions bilaterally (Fig. 4B, $P < 0.005$). Furthermore, we conducted statistical analysis to compare the differences of SI between left and right hemispheres. We found that SI in the right AI was significantly higher than SI in the left AI ($P < 0.01$, Fisher transform, 2-sample *t*-test). This result may indicate the differences of emotional processing in the left and right AI. After mapping the SI onto the average brain (Fig. 4C), we observed that the AI had much higher SI than the PI, indicating an increase in emotion selectivity from the PI to the AI. In Fig. 4D, the response amplitude (mean peak Z-score of broadband response to emotional sound stimuli of single electrode) is plotted against the SI for each electrode. HG and the PI have higher response amplitudes and weaker emotion selectivity, whereas the AI and amygdala have lower response amplitudes and stronger emotion selectivity (Fig. 4D). We further calculated response distances (see Supplementary Materials) between the 6 types of emotions (Fig. 4E). We defined the normalized response distance as the mean Euclidean distance of the broadband response to all emotion pairs across electrodes in HG, the PI, the AI, and the amygdala. We found that HG showed the smallest normalized response distance and that the amygdala showed the highest, with those of the PI and AI in between (Fig. 4E), which exhibited a gradient of emotion separability increasing from HG to the amygdala (the normalized response distance in the PI, the AI, and the amygdala were significant different from that in the HG, $P < 0.005$; the normalized response distance in the AI and the amygdala were significant different from that in the PI, $P < 0.01$; 2-sample *t*-test, Bonferroni correction). We also found that the emotion separability in the right

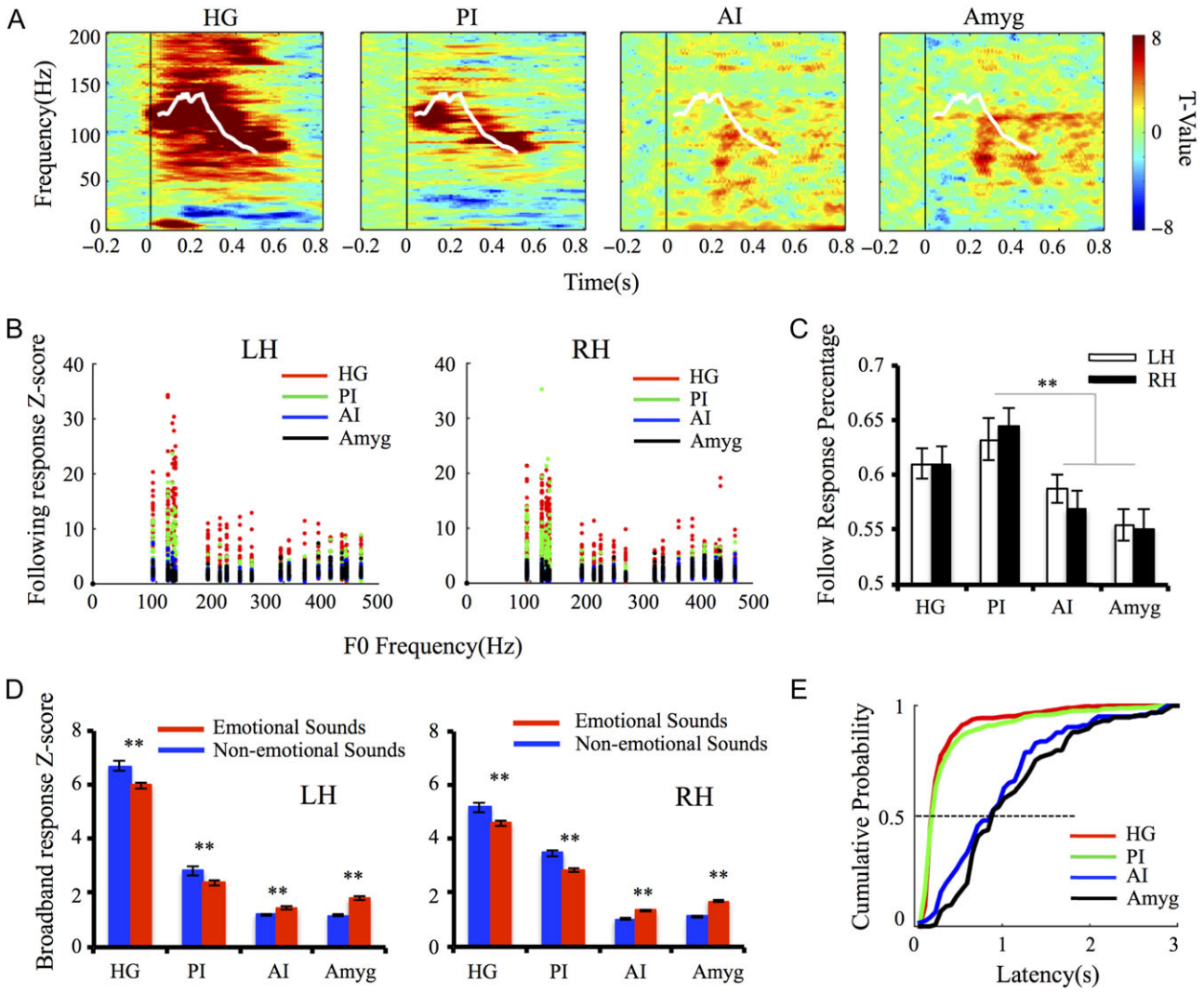

Figure 3. Cortical response patterns to emotional and nonemotional sounds: (*A*) Example response patterns of single electrodes in HG, PI, AI, and the amygdala (Amyg). White line inside each figure shows the pitch contour of the stimulus "disgust (2)". (*B*) Relationships between stimulus following response amplitude (Z-score) and the fundamental frequency (F_0) of the stimuli for HG, PI, AI, and Amyg in left hemisphere (LH) and right hemisphere (RH), respectively. (*C*) Percentage of energy of stimulus following response in HG, PI, AI, and Amyg in LH and RH. (**: $P < 0.01$, 2-sample *t*-test, Bonferroni correction). (*D*) Average broadband response amplitude to emotional and nonemotional sounds in HG, PI, AI, and Amyg in LH and RH, respectively. (**: $P < 0.01$, LH vs RH, 2-sample *t*-test.) (*E*) Cumulative distribution of the response latency of HG, PI, AI, and Amgy.

hemisphere was better or no worse than that of the left hemisphere (Fig. 4E, the HG and the amygdala had significant differences between left and right hemispheres, $P < 0.01$, 2-sample *t*-test). Taken together, we can conclude that the PI has no emotion selectivity, similar to HG, whereas the AI is an emotionally selective region, similar to the amygdala.

Electrical Stimulation of the Human Insula

In some of our patients, ECS was conducted in the insula to explore the epileptic zone and to identify critical functional areas. Using these data, we investigated the causal role of the insula in processing emotional sounds. We collected ECS data from 41 epilepsy patients with 233 electrodes that had contacts in the insula. This group of 41 patients (first 24 patients in Supplementary Table S2) included the 24 patients mentioned in the above sections (see Supplementary Fig. S1). ECS delivered to 104 (out of 233) electrodes evoked behavioral responses, which we defined as positive ECS responses (Fig. 5A), whereas stimulation to the rest 129 electrodes did not evoke obvious behaviors, which we defined as negative ECS responses (Fig. 5B). We further classified the patients' positive responses into auditory, sensorimotor, and autonomic responses (emotional processing); sign of seizure; or other types (see Supplementary Table S3). We focused on the analysis of auditory (Fig. 5C), sensorimotor (Fig. 5D), and autonomic (Fig. 5E) responses. As in iEEG analysis, resting fMRI data were used to parcellate the insula of each patient into the PI and AI regions. We found that electrodes with auditory responses were only located in the PI, whereas electrodes with autonomic responses were only located in the AI in both the left and right hemispheres (Fig. 5F,G). Additionally, we observed that the AI had a much higher ECS-negative response percentage (i.e., percentage of electrodes with negative responses) than the PI bilaterally (Fig. 5H). The electrical stimulation results further support the notion that the PI is a sensory region with sensory inputs

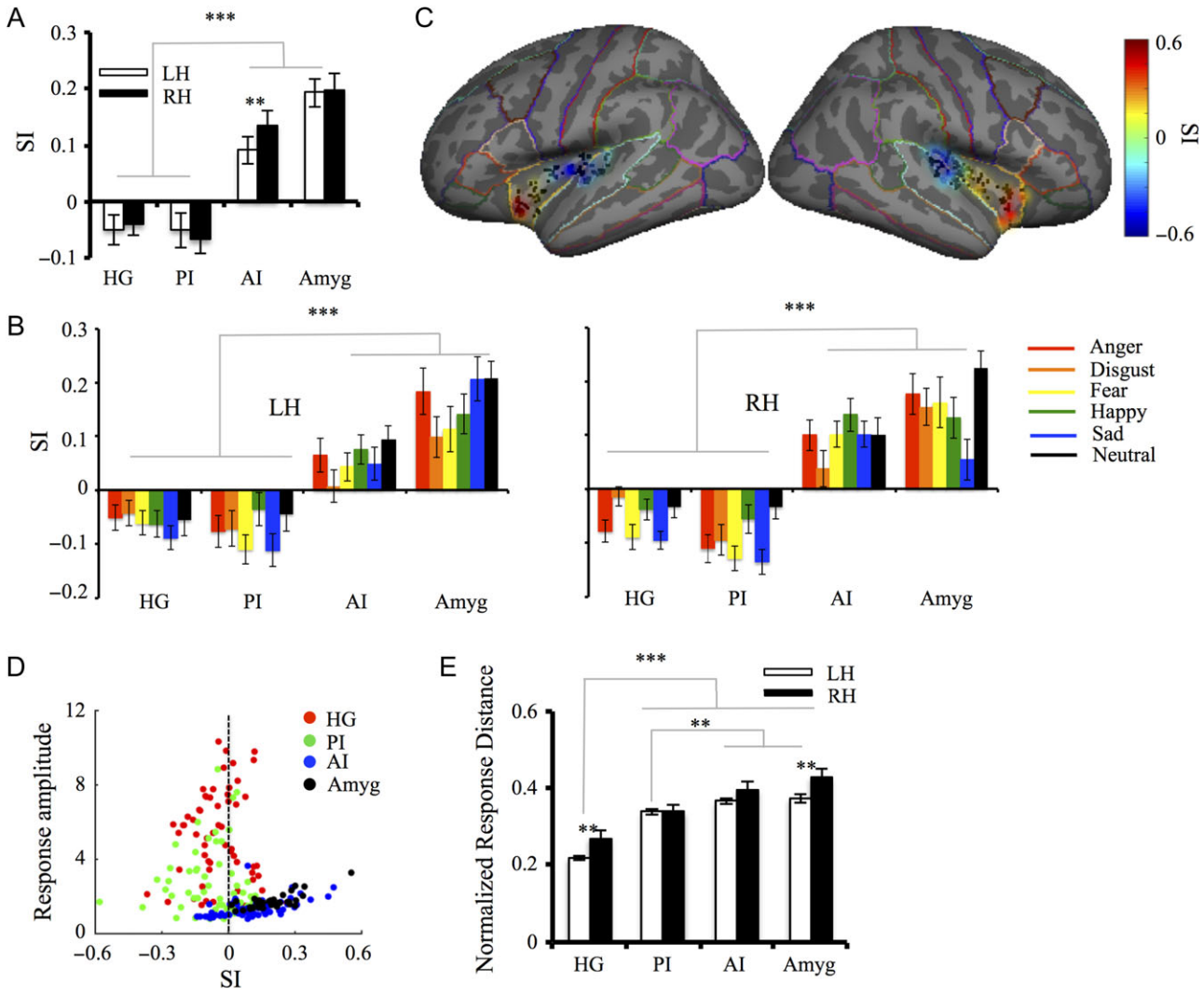

Figure 4. Emotion selectivity in the insula: (*A*) Average emotion SI of all electrodes in HG, PI, AI, and Amyg for LH and RH, respectively. (*B*) SI for 6 emotion types in LH and RH, respectively. (*C*) SI across all electrodes were mapped on the average brain for LH and RH, respectively. (*D*) Relationships between the broadband response amplitude and SI for every single electrode in HG, PI, AI, and Amyg. (*E*) Normalized response distance for all pairs of emotion types in HG, PI, AI, and Amyg for LH and RH, respectively. (*: $P < 0.05$; **: $P < 0.01$; ***: $P < 0.005$, 2-sample *t*-test, Bonferroni correction.)

and sensory neural responses, whereas the AI is a region with connections to/from the limbic system with emotional neural representations.

Discussion

In the present study, we utilized a multimodal approach involving DTI, resting fMRI, iEEG, and ECS to investigate the functional role of the human insula in auditory processing and emotion processing from auditory modality. First, structural and functional connectivity data both showed that the human insula is involved in 2 distinct neural networks, where the PI is primarily connected to visual, auditory, and sensorimotor cortices and the AI is primarily connected to frontal and cingulate cortices and the amygdala. Second, the PI is similar to HG, showing prominent responses to acoustic features of sound stimuli rather than emotional features, whereas the AI resembles the amygdala, which has stronger responses to emotional than nonemotional sounds. Third, from the PI to AI, an increasing gradient of the emotion SI was observed, along with an enlarged separability of the emotion types.

Auditory Field in the Posterior Insula

Our iEEG data revealed that recording sites in the PI responded to a wide variety of acoustic stimuli, with no preference to the emotional content. These results are in good agreement with the results from human imaging and lesion studies, which reported auditory agnosia following PI infarction (Augustine 1985; Habib et al. 1995; Bamiou et al. 2003; Wong et al. 2004; Bestelmeyer et al. 2014). In addition, the neurons recorded in the PI of macaque monkeys also exhibit auditory responses (Remedios et al. 2009), which may indicate the existence of an auditory field in the PI. Based on these results, an important question is raised: as the insula is not considered as a part of the central auditory nervous system, what is the functional role of the auditory field in PI? The present study cannot answer this question but can provide some insights. Tracing studies in non-human primates show dense connections between the PI and

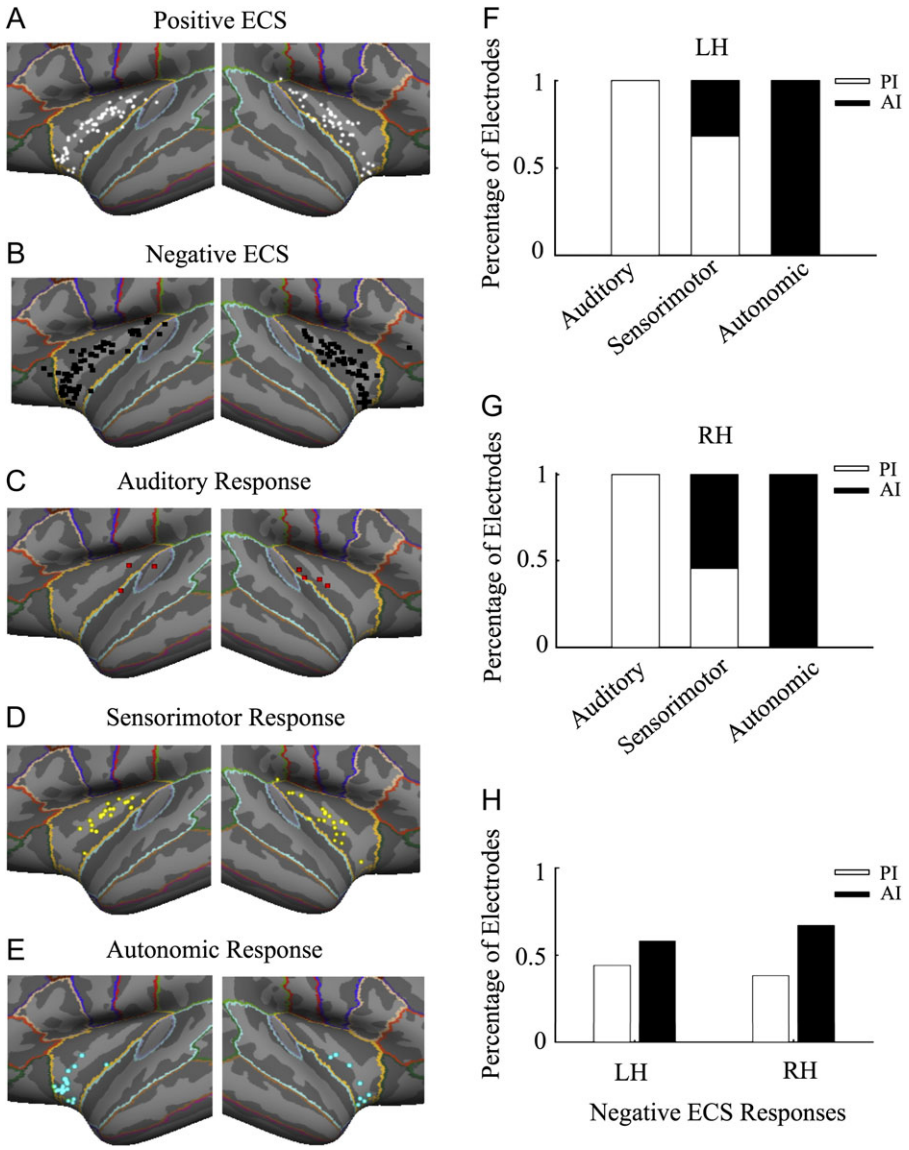

Figure 5. Insular sites responding to ECS: (*A–B*) Locations of electrodes with positive and negative ECS responses, respectively. (*C–E*) Locations of electrodes with auditory, sensorimotor, and autonomic responses, respectively. (*F–G*) Percentages of electrodes with auditory, sensorimotor, or autonomic responses in PI and AI of LH and RH, respectively. (*H*) Percentages of electrodes with negative ECS responses in PI and AI of LH and RH, respectively.

thalamic nuclei complexes, including the medial geniculate body (Burton and Jones 1976; Jones and Burton 1976), and dense connections between the PI and the auditory cortex (including HG) (Cauda et al. 2011; Cerliani et al. 2012; Cloutman et al. 2012; Dennis et al. 2014; Nomi et al. 2016). The strong connection between the PI and the auditory cortex was also found in the present study (Fig. 1C). We also found that the latency of neural activity in the PI was longer than that in HG (Fig. 3E), which indicated that the PI may receive auditory information from HG or the thalamus and might be involved in the network for processing auditory information. Additionally, we found that the neural responses in HG and PI tracked the F_0 of the stimuli and that the PI had an even higher following response percentage, which may indicate the role of the PI in extracting temporal features in sound. Bamiou et al. (2006) reported that patients with insular lesions exhibited deficits in auditory functions, especially in temporal resolution and sequencing, but with preserved cognitive functions. F_0 and amplitude envelope are important acoustic cues that convey emotional content (Schirmer and Kotz 2006; Sauter et al. 2010; Patel et al. 2011). Thus, the extraction of these cues in the PI may provide very useful information for further emotion processing in the AI and the amygdala.

Emotion Processing in the AI

Over the past several decades, a number of imaging and lesion studies have found that the AI is involved in a variety of functions, including processing affective and autonomic information (Oppenheimer et al. 1992; Phan et al. 2002; Barrett and Wager 2006; Afif et al. 2010; Lamm and Singer 2010; Caruana et al. 2011; Zaki et al. 2012). In addition, perceiving others' emotional states and feeling those emotions oneself can both activate the AI (Wicker et al. 2003; Singer et al. 2004; Hennenlotter et al. 2005; Corradi-Dell'Acqua et al. 2011; Lamm et al. 2011). These results

suggest that the AI is an important region to integrate external with internal emotional information to form a "global emotional moment" (Craig 2009). In this study, we found dense structural and functional connections of the AI with frontal, cingulate cortices and the amygdala, providing evidence that the AI is a part of the emotion-processing network. Compared with the PI, we found that the AI is selective to stimuli with emotional content, similar to the amygdala. However, the latency of the AI is slightly shorter than that of the amygdala (Fig. 3E), which may indicate interactions between the AI and the amygdala during the processing of the emotional content of auditory stimuli. In addition, we found that the response distances of different types of emotion were enlarged from the PI to AI, which may indicate that neuronal populations distributed along this axis have different emotion preferences. The iEEG electrodes used for recording may pick up the responses from several neuronal populations, thus showing different response patterns to different types of emotions.

Lateralization of the Insula

It has been suggested that emotional processing was mainly mediated by the right hemisphere (Harrington 1995). Recently, functional imaging studies have indicated that the left or right lateralization for emotional processing is determined by stimulus valence (positive or negative emotions) (Davidson et al. 1979; Hellige 1993), behavior (approach/withdrawal) (Davidson et al. 1990) or phenomenal state (perception/experience) (Garrett and Maddock 2006; Peelen et al. 2010; Zaki and Ochsner 2011). For the lateralization of the human insula, our findings provide the following insights: 1) we found significantly stronger connections between the insula and the amygdala in the right hemisphere than in the left hemisphere from our DTI results (Fig. 1C, subdivision 6); (2) we found a significantly higher emotion SI for the AI in the right hemisphere than in the left hemisphere (Fig. 4A); and (3) we observed that the response distances to different types of emotions for the AI were larger in the right hemisphere than in the left hemisphere (Fig. 4E). As our patients were all left language-dominated, these results suggest that language and emotion processing may be dominated by different hemispheres, which is consistent with the notion that the lateralization derives from the difference of stored representations in different hemispheres: left for lexical information and right for affective prosodic information (Hickok and Poeppel 2007).

Functional Role of the Insula

Functional imaging and electrical stimulation studies in human and nonhuman primates have suggested that the insula has a variety of functions. It has been suggested that the PI is involved in processing sensorimotor (Ostrowsky et al. 2002), auditory (Bamiou et al. 2003; Remedios et al. 2009; Chen et al. 2014), and visual information (Augustine 1996), whereas the AI is involved in processing pain (Brooks et al. 2005; Schweinhardt et al. 2006; Baliki et al. 2009; Wager et al. 2013), gustatory, olfactory (Augustine 1996; Shelley and Trimble 2004), interoceptive (Craig 2002, 2009; Critchley et al. 2004), affective (Phan et al. 2002; Barrett and Wager 2006; Lamm and Singer 2010; Caruana et al. 2011; Zaki et al. 2012), high-level cognitive (Sridharan et al. 2008; Menon and Uddin 2010), and autonomic information (Oppenheimer et al. 1992; Afif et al. 2010). Additionally, studies investigating the neural basis of empathy showed that witnessing others' emotional states recruited a network of brain areas, including the AI (Wicker et al. 2003; Singer et al. 2004; Hennenlotter et al. 2005; Corradi-Dell'Acqua et al. 2011; Lamm et al. 2011). The results of the present study provide new evidence to suggest a functional role of the insula in extracting the emotional content from auditory stimuli.

Humans are thought to differentiate among emotional states by interpreting external cues associated with a generalized internal physiological response that reflects changes in autonomic nervous system activity (James 1884; Dalgleish 2004). As the insula is an important site of multimodal convergence, Craig (Craig 2002) argued that it is the region for such integration. According to his theory, sensory information is conveyed to the PI, whereas affective information is represented in the AI via connections with the amygdala and the cingulate cortex. Our results support the idea that the PI is functionally and structurally connected to sensory cortices and has sensory representations, whereas the AI is connected to the limbic system and has affective representations. Thus, the insula resides at a suitable location for integrating internal and external information and for forming a global perception of how the self feels (Craig 2010).

Authors' Contributions

Y.Z., X.W., and B.H. conceived the experiments. Y.Z. performed experiments and data analysis. W.J.Z., Q.Z., H.X.W., and B.Q.Z. performed the neurosurgeries on the epilepsy patients and collected the ECS data. S.Y.W. collected the DTI data. J.H. and Y.Z. selected the emotional stimuli and designed the experimental paradigm. Y.Z., X.W., and B.H. wrote the manuscript.

Supplementary Material

Supplementary material is available at *Cerebral Cortex* online.

Funding

This work was supported by a grant from National Science Foundation of China (No. 61473169) and a grant from Tsinghua University.

Notes

We thank Y. Ding, H. Han, X.P. Si, C. Song, R. Xu, D. Zhang, and Y.L. Yan for comments and discussion. We thank H. Han for helping with the preprocessing of the fMRI data. We thank X.P. Si for providing the nonemotional sounds. *Conflict of Interest*: None declared.

References

Afif A, Minotti L, Kahane P, Hoffmann D. 2010. Anatomofunctional organization of the insular cortex: a study using intracerebral electrical stimulation in epileptic patients. Epilepsia. 51(11): 2305–2315.

Aggleton JP, Burton MJ, Passingham RE. 1980. Cortical and subcortical afferents to the amygdala of the rhesus monkey (Macaca mulatta). Brain Res. 190(2):347–368.

Allman JM, Tetreault NA, Hakeem AY, Manaye KF, Semendeferi K, Erwin JM, Park S, Goubert V, Hof PR. 2010. The von Economo neurons in frontoinsular and anterior cingulate cortex in great apes and humans. Brain Struct Funct. 214(5–6): 495–517.

Augustine JR. 1985. The insular lobe in primates including humans. Neurol Res. 7(1):2–10.

Augustine JR. 1996. Circuitry and functional aspects of the insular lobe in primates including humans. Brain Res Rev. 22(3): 229–244.

Baliki MN, Geha PY, Apkarian AV. 2009. Parsing pain perception between nociceptive representation and magnitude estimation. J Neurophysiol. 101(2):875–887.

Bamiou DE, Musiek FE, Luxon LM. 2003. The insula (Island of Reil) and its role in auditory processing: literature review. Brain Res Rev. 42(2):143–154.

Bamiou DE, Musiek FE, Stow I, Stevens J, Cipolotti L, Brown MM, Luxon LM. 2006. Auditory temporal processing deficits in patients with insular stroke. Neurology. 67(4):614–619.

Barrett LF, Wager TD. 2006. The structure of emotion evidence from neuroimaging studies. Curr Dir Psychol Sci. 15(2):79–83.

Belin P, Fillion-Bilodeau S, Gosselin F. 2008. The Montreal Affective Voices: a validated set of nonverbal affect bursts for research on auditory affective processing. Behav Res Methods. 40(2):531–539.

Bestelmeyer PE, Maurage P, Rouger J, Latinus M, Belin P. 2014. Adaptation to vocal expressions reveals multistep perception of auditory emotion. J Neurosci. 34(24):8098–8105.

Brainard DH. 1997. The psychophysics toolbox. Spat Vis. 10: 433–436.

Brooks JCW, Zambreanu L, Godinez A, Tracey I. 2005. Somatotopic organisation of the human insula to painful heat studied with high resolution functional imaging. Neuroimage. 27(1):201–209.

Burton H, Jones EG. 1976. The posterior thalamic region and its cortical projection in New World and Old World monkeys. J Comp Neurol. 168(2):249–301.

Caruana F, Jezzini A, Sbriscia-Fioretti B, Rizzolatti G, Gallese V. 2011. Emotional and social behaviors elicited by electrical stimulation of the insula in the macaque monkey. Curr Biol. 21(3):195–199.

Cauda F, D'Agata F, Sacco K, Duca S, Geminiani G, Vercelli A. 2011. Functional connectivity of the insula in the resting brain. Neuroimage. 55(1):8–23.

Cerliani L, Thomas RM, Jbabdi S, Siero JC, Nanetti L, Crippa A, Gazzola V, D'Arceuil H, Keysers C. 2012. Probabilistic tractography recovers a rostrocaudal trajectory of connectivity variability in the human insular cortex. Hum Brain Mapp. 33 (9):2005–2034.

Chen C, Lee YH, Cheng Y. 2014. Anterior insular cortex activity to emotional salience of voices in a passive oddball paradigm. Front Hum Neurosci. 8:743.

Cloutman LL, Binney RJ, Drakesmith M, Parker GJ, Ralph MAL. 2012. The variation of function across the human insula mirrors its patterns of structural connectivity: evidence from in vivo probabilistic tractography. Neuroimage. 59(4): 3514–3521.

Corradi-Dell'Acqua C, Hofstetter C, Vuilleumier P. 2011. Felt and seen pain evoke the same local patterns of cortical activity in insular and cingulate cortex. J Neurosci. 31(49): 17996–18006.

Craig AD. 2002. How do you feel? Interoception: the sense of the physiological condition of the body. Nat Rev Neurosci. 3 (8):655–666.

Craig AD. 2009. How do you feel—now? The anterior insula and human awareness. Nat Rev Neurosci. 10(1):59–70.

Craig AD. 2010. The sentient self. Brain Struct Funct. 214: 563–577.

Critchley HD, Wiens S, Rotshtein P, Öhman A, Dolan RJ. 2004. Neural systems supporting interoceptive awareness. Nat Neurosci. 7(2):189–195.

Cui Z, Zhong S, Xu P, He Y, Gong G. 2013. PANDA: a pipeline toolbox for analyzing brain diffusion images. Front Hum Neurosci. 7:42.

Dalgleish T. 2004. The emotional brain. Nat Rev Neurosci. 5(7): 583–589.

Damoiseaux JS, Rombouts SARB, Barkhof F, Scheltens P, Stam CJ, Smith SM, Beckmann CF. 2006. Consistent resting-state networks across healthy subjects. Proc Nat Acad Sci USA. 103(37):13848–13853.

Davidson RJ, Ekman P, Saron CD, Senulis JA, Friesen WV. 1990. Approach-withdrawal and cerebral asymmetry: emotional expression and brain physiology: I. J Pers Soc Psychol. 58(2):330.

Davidson RJ, Schwartz GE, Saron C, Bennett J, Goleman DJ. 1979. Frontal versus parietal EEG asymmetry during positive and negative affect. Psychophysiology. 16(2):202–203.

Dennis EL, Jahanshad N, McMahon KL, Zubicaray GI, Martin NG, Hickie IB, Toga AW, Wright MJ, Thompson PM. 2014. Development of insula connectivity between ages 12 and 30 revealed by high angular resolution diffusion imaging. Hum Brain Mapp. 35(4):1790–1800.

Fan L, Li H, Zhuo J, Zhang Y, Wang J, Chen L, Yang Z, Chu C, Xie S, Laird AR, et al. 2016. The Human Brainnetome Atlas: a new brain atlas based on connectional architecture. Cereb Cortex. 26(8):3508–3526.

Flynn FG. 1999. Anatomy of the insula functional and clinical correlates. Aphasiology. 13(1):55–78.

Fox MD, Snyder AZ, Vincent JL, Corbetta M, Van Essen DC, Raichle ME. 2005. The human brain is intrinsically organized into dynamic, anticorrelated functional networks. Proc Nat Acad Sci USA. 102(27):9673–9678.

Garrett AS, Maddock RJ. 2006. Separating subjective emotion from the perception of emotion-inducing stimuli: an fMRI study. Neuroimage. 33(1):263–274.

Greicius MD, Krasnow B, Reiss AL, Menon V. 2003. Functional connectivity in the resting brain: a network analysis of the default mode hypothesis. Proc Nat Acad Sci USA. 100(1): 253–258.

Griffiths TD, Kumar S, Sedley W, Nourski KV, Kawasaki H, Oya H, Patterson RD, Brugge JF, Howard MA. 2010. Direct recordings of pitch responses from human auditory cortex. Curr Biol. 20(12):1128–1132.

Habib M, Daquin G, Milandre L, Royere ML, Rey M, Lanteri A, Salamon G, Khalil R. 1995. Mutism and auditory agnosia due to bilateral insular damage—role of the insula in human communication. Neuropsychologia. 33(3):327–339.

Hampson M, Peterson BS, Skudlarski P, Gatenby JC, Gore JC. 2002. Detection of functional connectivity using temporal correlations in MR images. Hum Brain Mapp. 15(4): 247–262.

Harrington A. 1995. Unfinished business: models of laterality in the nineteenth century. In Davidson RJ, Hugdahl K, editors. Cambridge (MA): Brain Asymmetry, MIT Press. p. 3–27.

Hellige JB. 1993. Hemispheric asymmetry: what's right and what's left. Vol. 6. Cambridge (MA): Harvard University Press.

Hennenlotter A, Schroeder U, Erhard P, Castrop F, Haslinger B, Stoecker D, Lange KW, Ceballos-Baumann AO. 2005. A common neural basis for receptive and expressive communication of pleasant facial affect. Neuroimage. 26(2):581–591.

Hickok G, Poeppel D. 2007. The cortical organization of speech processing. Nat Rev Neurosci. 8(5):393–402.

Höistad M, Barbas H. 2008. Sequence of information processing for emotions through pathways linking temporal and insular cortices with the amygdala. Neuroimage. 40(3):1016–1033.

James W. 1884. What is an emotion? Mind. 34:188–205.
Jones EG, Burton H. 1976. Areal differences in the laminar distribution of thalamic afferents in cortical fields of the insular, parietal and temporal regions of primates. J Comp Neurol. 168(2):197–247.
Lamm C, Decety J, Singer T. 2011. Meta-analytic evidence for common and distinct neural networks associated with directly experienced pain and empathy for pain. Neuroimage. 54(3): 2492–2502.
Lamm C, Singer T. 2010. The role of anterior insular cortex in social emotions. Brain Struct Funct. 214(5–6):579–591.
Menon V, Uddin LQ. 2010. Saliency, switching, attention and control: a network model of insula function. Brain Struct Funct. 214(5–6):655–667.
Mesulam M, Mufson EJ. 1982. Insula of the old world monkey. Architectonics in the insulo-orbito-temporal component of the paralimbic brain. J Comp Neurol. 212(1):1–22.
Mesulam MM, Mufson EJ. 1985. The insula of Reil in man and monkey: Architectonics, connectivity, and function. In: Peters A, Jones EG, editors. Cereb Cortex, Vol. 4. Association and auditory cortices. New York: Plenum. p. 179–226.
Mufson EJ, Mesulam MM, Pandya DN. 1981. Insular interconnections with the amygdala in the rhesus monkey. Neuroscience. 6(7):1231–1248.
Nomi JS, Farrant K, Damaraju E, Rachakonda S, Calhoun VD, Uddin LQ. 2016. Dynamic functional network connectivity reveals unique and overlapping profiles of insula subdivisions. Hum Brain Mapp. 37:1770–1787.
Oppenheimer SM, Gelb A, Girvin JP, Hachinski VC. 1992. Cardiovascular effects of human insular cortex stimulation. Neurology. 42(9):1727–1727.
Ostrowsky K, Magnin M, Ryvlin P, Isnard J, Guenot M, Mauguière F. 2002. Representation of pain and somatic sensation in the human insula: a study of responses to direct electrical cortical stimulation. Cereb Cortex. 12(4): 376–385.
Pandya DN, Karol EA, Heilbronn D. 1971. The topographical distribution of interhemispheric projections in the corpus callosum of the rhesus monkey. Brain Res. 32(1):31–43.
Pandya DN, Rosene DL. 1985. Some observations on trajectories and topography of commissural fibres. In: Reeves AG, editor. Epilepsy and the corpus callosum. New York: Plenum. p. 21–39.
Patel S, Scherer KR, Björkner E, Sundberg J. 2011. Mapping emotions into acoustic space: the role of voice production. Biol Psychol. 87(1):93–98.
Peelen MV, Atkinson AP, Vuilleumier P. 2010. Supramodal representations of perceived emotions in the human brain. J Neurosci. 30(30):10127–10134.
Phan KL, Wager T, Taylor SF, Liberzon I. 2002. Functional neuroanatomy of emotion: a meta-analysis of emotion activation studies in PET and fMRI. Neuroimage. 16(2):331–348.
Remedios R, Logothetis NK, Kayser C. 2009. An auditory region in the primate insular cortex responding preferentially to vocal communication sounds. J Neurosci. 29(4): 1034–1045.
Rivier F, Clarke S. 1997. Cytochrome oxidase, acetylcholinesterase, and NADPH-diaphorase staining in human supratemporal and insular cortex: evidence for multiple auditory areas. Neuroimage. 6(4):288–304.
Rose M. 1928. Die inselrinde des menschen und der tiere. J Psychol Neurol. 37:467–624.
Sauter DA, Eisner F, Calder AJ, Scott SK. 2010. Perceptual cues in nonverbal vocal expressions of emotion. Q J Exp Psychol. 63 (11):2251–2272.
Schirmer A, Kotz SA. 2006. Beyond the right hemisphere: brain mechanisms mediating vocal emotional processing. Trends Cogn Sci. 10(1):24–30.
Schweinhardt P, Glynn C, Brooks J, McQuay H, Jack T, Chessell I, Bountra C, Tracey I. 2006. An fMRI study of cerebral processing of brush-evoked allodynia in neuropathic pain patients. Neuroimage. 32(1):256–265.
Shelley BP, Trimble MR. 2004. The insular lobe of Reil—its anatamico-functional, behavioural and neuropsychiatric attributes in humans—a review. World J Biol Psychiatry. 5 (4):176–200.
Singer T, Seymour B, O'doherty J, Kaube H, Dolan RJ, Frith CD. 2004. Empathy for pain involves the affective but not sensory components of pain. Science. 303(5661):1157–1162.
Smolders A, De Martino F, Staeren N, Scheunders P, Sijbers J, Goebel R, Formisano E. 2007. Dissecting cognitive stages with time-resolved fMRI data: a comparison of fuzzy clustering and independent component analysis. Magn Reson Imaging. 25(6):860–868.
Sridharan D, Levitin DJ, Menon V. 2008. A critical role for the right fronto-insular cortex in switching between central-executive and default-mode networks. Proc Nat Acad Sci USA. 105(34):12569–12574.
Turner BH, Mishkin M, Knapp M. 1980. Organization of the amygdalopetal projections from modality-specific cortical association areas in the monkey. J Comp Neurol. 191(4):515–543.
Vincent JL, Patel GH, Fox MD, Snyder AZ, Baker JT, Van Essen DC, Zempel JM, Snyder LH, Corbetta M, Raichle ME. 2007. Intrinsic functional architecture in the anaesthetized monkey brain. Nature. 447(7140):83–86.
von Economo CF, Koskinas GN 1925. Die Cytoarchitektonik der Hirnrinde des erwachsenen Menschen. Springer, Berlin.
Wager TD, Atlas LY, Lindquist MA, Roy M, Woo CW, Kross E. 2013. An fMRI-based neurologic signature of physical pain. N Engl J Med. 368(15):1388–1397.
Wang D, Buckner RL, Fox MD, Holt DJ, Holmes AJ, Stoecklein S, Langs G, Pan R, Qian T, Li K, et al. 2015. Parcellating cortical functional networks in individuals. Nat Neurosci. 18(12): 1853–1860.
Wicker B, Keysers C, Plailly J, Royet JP, Gallese V, Rizzolatti G. 2003. Both of us disgusted in my insula: the common neural basis of seeing and feeling disgust. Neuron. 40(3):655–664.
Wong PC, Parsons LM, Martinez M, Diehl RL. 2004. The role of the insular cortex in pitch pattern perception: the effect of linguistic contexts. J Neurosci. 24(41):9153–9160.
Zaki J, Davis JI, Ochsner KN. 2012. Overlapping activity in anterior insula during interoception and emotional experience. Neuroimage. 62(1):493–499.
Zaki J, Ochsner KN. 2011. You, me, and my brain: self and other representation in social cognitive neuroscience. Soc Neurosci. 26:48.